

The interleukin-1 axis and the tumor immune microenvironment in pancreatic ductal adenocarcinoma



Kelly M. Herremans^a; Dominique D. Szymkiewicz^a;
Andrea N. Riner^a; Riley P. Bohan^a;
Gerik W. Tushoski^a; Aaron M. Davidson^a;
XiangYang Lou^b; Man Chong Leong^b;
Bayli DiVita Dean^c; Michael Gerber^a;
Patrick W. Underwood^a; Song Han^a;
Steven J. Hughes^{a,*}

^a Department of Surgery, University of Florida College of Medicine, P.O. Box 100109, Gainesville, FL 32610, USA

^b Department of Biostatistics, University of Florida College of Medicine, P.O. Box 117450, Gainesville, FL 32611-7450, USA

^c Preston A. Wells, Jr. Center for Brain Tumor Therapy, Lillian S. Wells Department of Neurosurgery, University of Florida Brain Tumor Immunotherapy Program, University of Florida, 1149 S Newell Dr, L2-100, Gainesville, FL 32611, USA

Abstract

Interleukin-1 (IL-1) plays a key role in carcinogenesis and several IL-1-targeted therapeutics are under investigation for the treatment of pancreatic ductal adenocarcinoma (PDAC). We sought to broaden our understanding of how the family of IL-1 ligands and receptors impact the tumor immune landscape and patient survival in PDAC. Gene expression data and DNA methylation data for IL1A, IL1B, IL1RN, IL1R1, IL1R2, and IL1RAP was attained from The Cancer Genome Atlas (TCGA) database and cross validated using the National Center for Biotechnology Information (NCBI) Gene Expression Omnibus (GEO) database. Immune cell-type abundance was estimated using CIBERSORTx. Further confirmatory soluble protein analysis and peripheral blood immunophenotyping were performed on available tissue samples from our institution. 169 PDAC patients and 50 benign pancreatic TCGA-based samples were analyzed. IL1A ($p < 0.001$), IL1RN ($p < 0.001$), IL1R2 ($p < 0.001$), and IL1RAP ($p = 0.006$) were markedly increased in PDAC tumor tissue compared to benign pancreatic tissue. Furthermore, expression of IL1A, IL1B and IL1R1 were positively correlated with gene expression of immune checkpoints PVR, CD274, CD47, CD80, and HLA-A/B/C ($p < 0.001$). IL1B and IL1R1 were correlated to expression of PDCD1, CD86, CTLA4 and IDO1 (< 0.001). Low expression of IL1RN ($p = 0.020$), IL1R2 ($p = 0.015$), and IL1RAP ($p = 0.003$) and high expression of IL1B ($p = 0.031$) were correlated with increased patient survival. At the protein level, IL-1 β was correlated with increased peripheral central memory CD4+ and CD8+ T-cells as well as decreased Th2 cells. These findings suggest that the IL-1 axis plays a complex and pivotal role in the host immune response to PDAC.

Neoplasia (2022) 28, 100789

Keywords: Pancreas cancer, Bioinformatics, Immunology, Immune checkpoint, Survival

Abbreviations: PDAC, pancreatic ductal adenocarcinoma; IL-1, interleukin-1; IL-1R₁, interleukin-1 receptor 1; IL-1R₂, interleukin-1 receptor 2; IL-1Ra, interleukin-1 receptor antagonist; IL-1RAP, interleukin-1 receptor accessory protein; TCGA, the cancer genome atlas; PAAD, pancreatic adenocarcinoma; NCBI, National Center for Biotechnology Information; GEO, gene expression omnibus; PVR, poliovirus receptor; CD, cluster of differentiation; HLA, human leukocyte antigen; IDO1, Indoleamine 2,3-dioxygenase 1; LIF, leukemia inhibitory factor.

* Corresponding author.

E-mail address: Steven.Hughes@surgery.ufl.edu (S.J. Hughes).

Received 13 January 2022; received in revised form 14 March 2022; accepted 17 March 2022

© 2022 The Authors. Published by Elsevier Inc.
This is an open access article under the CC BY-NC-ND license
<http://creativecommons.org/licenses/by-nc-nd/4.0/>
<https://doi.org/10.1016/j.neo.2022.100789>

Introduction

Projected to become the second leading cause of cancer death within the decade, pancreatic ductal adenocarcinoma (PDAC) remains a deadly disease with limited effective treatment options [1]. PDAC is particularly resistant to systemic cytotoxic and kinase-targeted therapeutics, leaving patients with an estimated 5-year survival of 11% [2]. Though the implementation of immunotherapies has been successful in other cancer types [3,4], they have shown negligible effect in the treatment of PDAC. This is in part due to its inherently immunosuppressive tumor microenvironment [5–7].

More recently, attention has turned toward understanding the interplay between inflammation and anti-tumor immune response. The interleukin-1

(IL-1) family of cytokines plays a key role in modulating both the innate and adaptive immune response [8]. The proinflammatory IL-1 α (IL1A) and IL-1 β (IL1B) ligands bind to the IL-1R₁ receptor (IL1R1), though the accessory protein IL-1R₃ (IL1RAP) is required for signal propagation. Conversely, IL-1Ra (IL1RN) serves as an antagonist binding to IL-1R₁ to inhibit further signaling. Additionally, IL-1R₂ (IL1R2) is a decoy receptor that does not result in signal transduction [9]. Dysregulation of this pathway has been implicated in a number of autoimmune and inflammatory diseases, but understanding of its role in cancer is still rudimentary.

The importance of IL-1 family members has been illustrated across a number of different cancer types including thyroid, ovarian, gastric, lung, prostate as well as pancreatic cancer [10]. In previous work, our group reported the diagnostic utility of IL-1Ra as it significantly differentiated benign pancreatic tissue from PDAC [11]. We also noted that IL-1 β was associated with poor histologic response to neoadjuvant therapy [12]. Additional studies exhibited promising results in murine models using recombinant IL-1Ra (anakinra), leading to attenuated tumor growth [13]. These findings prompted the application of anakinra as a combination therapy with chemotherapeutics in PDAC clinical trials [14]. Despite this progress, little remains known about how the totality of the IL-1 axis influences the tumor immune microenvironment in human samples. Using a bioinformatics approach, we aimed to explore how the IL-1 axis changes in PDAC carcinogenesis and impacts the immune milieu of the human PDAC tumor microenvironment.

Materials and methods

Data availability

Data were obtained through the National Cancer Institute Genomic Data Commons database utilizing The Cancer Genome Atlas (TCGA) pancreatic adenocarcinoma (PAAD) dataset. Tumor samples were excluded from analysis if they were a neuroendocrine carcinoma subtype ($n = 9$), mucinous non-cystic carcinoma ($n = 4$) and undifferentiated carcinoma ($n = 1$). Patient data including demographics, treatment type, clinical outcomes, and follow-up were obtained through the TCGA-PAAD database.

Confirmatory gene expression data were obtained through the National Center for Biotechnology Information (NCBI) Gene Expression Omnibus (GEO) database [15]. Using reference series GSE16515 and GSE28735, gene expression profiles were evaluated for PDAC and normal pancreatic tissue [16,17]. This study was approved through the University of Florida Institutional Review Board (IRB202101243).

Gene expression and DNA methylation analysis

Data were obtained from TCGA-PAAD for the gene expression and methylation of IL1A, IL1B, IL1RN, IL1R1, IL1R2 and IL1RAP and verified using GEO datasets. Comparative analysis between tumor samples and normal tissue was performed for the gene expression and methylation of IL1A, IL1B, IL1RN, IL1R1, IL1R2 and IL1RAP with the TCGA-PAAD data and verified with the GEO database using a two-tail, two-sample, unequal variance t-test with a significance level of $\alpha=0.05$.

Gene correlation analysis

Spearman correlation analysis was performed between members of the IL-1 axis in order to assess for correlation of gene expression within the TCGA-PAAD dataset. Spearman correlation was also used to assess correlation between gene expression and methylation within the TCGA- PAAD dataset.

Table 1

Patient demographics and pathologic stage of The Cancer Genome Atlas pancreatic ductal adenocarcinoma samples (TCGA-PAAD) ($n = 169$).

Characteristics	Mean (SD) or % (n)
Age	
Average Age at Diagnosis (years)	65.6
Gender	
Male	55.0% (93)
Female	45.0% (76)
Race	
White	87.6% (148)
Asian	6.5% (11)
African American	3.6% (6)
Not reported	2.4% (4)
Ethnicity	
Not Hispanic or Latinx	72.8% (123)
Hispanic or Latinx	3.0% (5)
Not reported	24.3% (41)
Stage	
Stage Ia	3.0% (5)
Stage Ib	5.9% (10)
Stage IIa	16.6% (28)
Stage IIb	69.2% (117)
Stage III	1.8% (3)
Stage IV	2.4% (4)
Not reported	1.2% (2)

Immune cell composition

Immune cell types were estimated using CIBERSORTx as previously described by Thorsson et al. [18]. CIBERSORTx is an analytical tool used to provide an estimation of cell type abundance through the analysis of gene expression data [19]. CIBERSORTx was applied to the TCGA RNAseq database in order to identify the relative proportion of immune cell types.

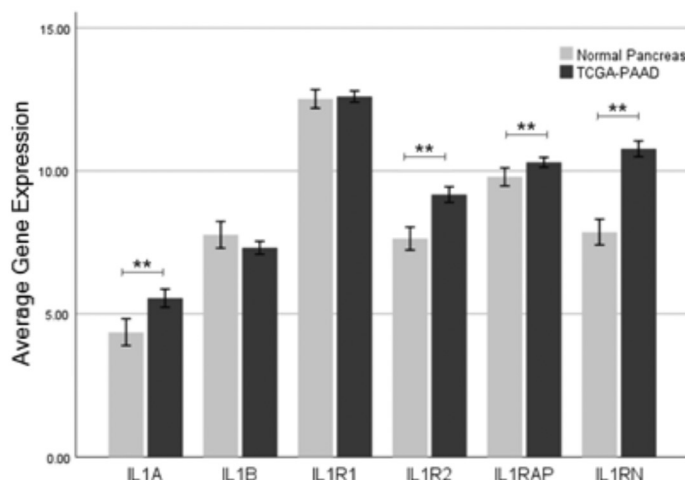
Survival analysis

High and low gene expression was defined by *Cutoff Finder* (https://molpathoheidelberg.shinyapps.io/CutoffFinder_v1/) as described by Budczies et al. *Cutoff finder* is a comprehensive tool used to optimize the analysis of gene expression for cutoff determination [21]. Kaplan Meier survival analysis was utilized to compare high and low gene expression groups using $p < 0.05$ for statistical significance.

Tumor microenvironment soluble analysis

Tissue samples were obtained from patients with confirmed PDAC through a prospectively maintained tissue bank at the University of Florida (IRB201600873) from October 14 2011 to April 23, 2018. Patients were excluded if they did not have matched peripheral blood immunophenotyped samples. Tumor samples were stored immediately following surgical resection and flash frozen in liquid nitrogen within twenty minutes of resection and stored at -80°C . At the time of processing, tumors underwent homogenization and were then probed for IL-1 analytes using a commercially available multiplex assay per the manufacturer's protocol (Catalog# HCYTMAG-60K-PX41, Millipore Sigma, Burlington, MA, USA) and as previously described [11].

A)



B)

	IL1A	IL1B	IL1R1	IL1R2	IL1RAP	IL1RN
GSE16515	1.06**	0.49	-0.25	2.13**	1.56**	1.29**
GSE28735	0.53**	-0.50**	0.04	1.04**	1.10**	0.96**

Fig. 1. (A) Gene expression differences in normal pancreatic tissue ($n = 50$) compared to pancreatic tumor samples ($n = 169$), where * denotes significance of p -value < 0.05 and ** denotes significance of p -value < 0.01 . The error bars represent 95% confidence interval. (B) Confirmatory analysis using the GEO database. Log fold change in pancreatic tumor versus control tissue where positive fold change denotes an increase in expression from control to tumor.

Peripheral immunophenotype

Matched samples of patient peripheral blood mononuclear cells were identified and immunostained. They were subjected to flow cytometer analysis to determine population frequencies of immune cell types and immune checkpoint proteins per the established protocol [20]. Spearman correlation was then utilized to assess correlations between the tumor microenvironment and peripheral immunophenotype.

Results

Gene expression of the IL1 family of ligands and receptors

Through an analysis of 169 PDAC and 50 benign samples from the TCGA database (Table 1), gene expression levels of the IL-1 family were evaluated. When compared to benign pancreatic tissue, PDAC tumors were found to have significantly higher gene expression of IL1A ($p < 0.001$), IL1RN ($p < 0.001$), IL1R2 ($p < 0.001$) and IL1RAP ($p = 0.006$) (Fig. 1A). No statistically significant differences were found between IL1B and IL1R1 gene expression. These data were then subsequently confirmed using GEO datasets GSE16515 and GSE28735. GSE16515 includes 36 PDAC and 16 benign samples, whereas GSE28735 includes 45 PDAC and 45 benign samples (Fig. 1B). In addition to confirming the differences noted above, gene expression levels of IL1B were found to be lower in PDAC when compared to benign tissue ($p = 0.026$) in the latter analysis.

DNA methylation of the IL-1 axis

In order to further assess how DNA methylation regulates expression of the IL-1 axis, DNA methylation levels of IL1A, IL1B, IL1RN, IL1R1, IL1R2 and IL1RAP were analyzed (Fig. 2). When compared to benign

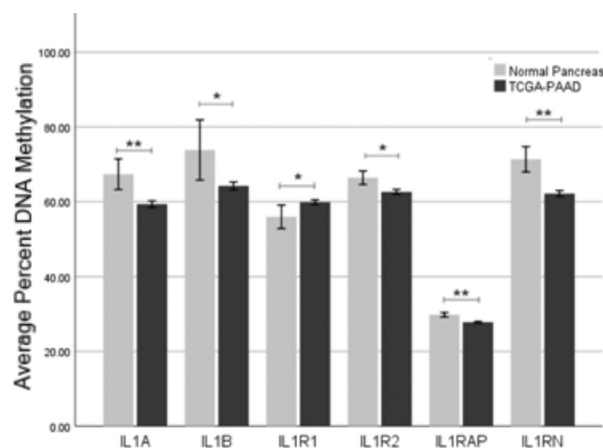


Fig. 2. DNA methylation differences comparing pancreatic tumor samples to normal pancreas samples, where * denotes significance of p -value < 0.05 and ** denotes significance of p -value < 0.01 . Error bars represent 95% confidence interval.

samples, DNA methylation levels of PDAC samples were decreased in IL1A ($p = 0.001$), IL1B ($p = 0.014$), IL1RN ($p < 0.001$), IL1RAP ($p < 0.001$) and IL1R2 ($p = 0.024$). Additionally, PDAC samples showed evidence of increased DNA methylation of IL1R1 when compared to benign samples ($p = 0.014$). To evaluate the correlative strength between DNA methylation and gene expression within PDAC samples alone, Spearman analysis was performed for each member of the IL-1 axis (Fig. S1). The DNA methylation of IL1B ($p = 0.008$, $\rho = -0.202$) and IL1R2 ($p = 0.022$, $\rho = 0.176$) correlated significantly with DNA expression. However, DNA methylation

and expression of IL1A ($p = 0.604$, $\rho = [-0.040]$), IL1RN ($p = 0.216$, $\rho = [-0.096]$), IL1R1 ($p = 0.537$, $\rho = [-0.048]$), IL1RAP ($p = 0.658$, $\rho = [0.034]$) were not correlative.

The interplay of the IL-1 axis in PDAC

To better understand the relationships within the IL-1 axis, correlations between IL-1 genes within PDAC samples were assessed using Spearman analysis (Fig. S2). The gene expression of IL1A was found to be correlated with IL1B ($p < 0.001$, $\rho = [0.342]$), IL1RN ($p < 0.001$, $\rho = [0.377]$), IL1R2 ($p < 0.001$, $\rho = [0.283]$) and IL1RAP ($p < 0.001$, $\rho = [0.385]$) but not IL1R1 ($p = 0.231$, $\rho = [-0.028]$). IL1B gene expression was also correlated to IL1R1 ($p < 0.001$, $\rho = 0.429$) and IL1RAP ($p < 0.001$, $\rho = 0.239$) though was not correlated to IL1R2 ($p = 0.397$, $\rho = [0.066]$) or IL1RN ($p = 0.275$, $\rho = [0.084]$). Additionally, IL1R1 gene expression was significantly correlated to IL1RAP ($p < 0.001$, $\rho = [0.393]$) but not IL1R2 ($p = 0.761$, $\rho = [0.024]$) or IL-1RN ($p = 0.809$, $\rho = [0.019]$) expression. IL1R2 gene expression was correlated with IL1RAP ($p = 0.042$, $\rho = [0.156]$) and IL1RN ($p < 0.001$, $\rho = [0.553]$). IL1RAP gene expression was correlated to IL1RN ($p < 0.001$, $\rho = [0.379]$).

The tumor immune microenvironment

In order to analyze how the IL-1 axis impacts the tumor immune microenvironment, gene expression was correlated to immune cell type abundance within PDAC samples (Table 2). Expression of IL1A, which is increased in PDAC samples, was significantly associated with increased T helper type 1 cells (Th1), total macrophages, non-activated (M0) macrophages, neutrophils, and eosinophils. Conversely, IL1A was significantly associated with a decreased composition of T helper 17 cells (Th17) and mast cells. IL1B expression was associated with an increased abundance of Th1 cells and neutrophils, but also to increased resting CD4+ T-cells and T regulatory cells. Expression of IL1B was also associated with a decrease in memory B cells and plasma B cells.

Expression of IL1R1, the receptor of the IL-1 α and IL-1 β ligands, was also associated with an increased abundance of Th1 cells, as well as naïve B cells, activated and resting memory CD4+ T cells, CD8+ T cells, eosinophils, mast cells, and dendritic cells. IL1R1 expression was associated with a decreased abundance Th17 cells, memory B cells, M0 macrophages, plasma B cells, and T regulatory cells. Expression of IL1R2, which codes for the decoy receptor IL-1R $_2$, was associated only with an increased abundance of Th2 cells and eosinophils. Expression of IL1RAP, the accessory protein to IL-1R $_1$ required for signal initiation similarly showed evidence of increased eosinophils as well as increased Th2 cells, overall macrophages, and neutrophils. Expression of IL1RAP was also associated with a decreased abundance of Th17 cells, memory B cells, plasma B cells, gamma T cells, T regulatory cells and lymphocytes. The expression of IL1RN, which encodes for the antagonist to IL-1 α and IL-1 β , was associated with increased abundance of both M1 macrophages and M2 macrophages as well as increased T regulatory cells, neutrophils and dendritic cells. Conversely, IL1RN was associated with a decrease in naïve B cells and naïve CD4 T cells.

Peripheral immunophenotype

Given the limitations of publicly available datasets to assess the impact of the IL1 family on the circulating immune response, we compared the levels of the proteins IL-1 α , IL-1 β and IL-1Ra within the tumor microenvironment to the peripheral blood immunophenotype of 17 patients within our institution (Supp Table 1). In 17 matched samples, we found the IL-1 β within the tumor microenvironment was associated with an increased levels of both central memory CD4+ T cells as well as central memory CD8+ T cells. Furthermore, IL-1 β was inversely associated with T helper 2 (Th2) cells

Table 2

Spearman two-tailed correlations between gene expression of IL1A, IL1B, IL1R1, IL1R2, IL1RAP, IL1RN and immune cell gene expression in 169 TCGA-PAAD patients. Green coloring emphasizes increase, red emphasizes decrease, * signifies $p < 0.05$ and ** signifies $p < 0.01$.

	IL1A rho	IL1B rho	IL1R1 rho	IL1R2 rho	IL1RAP rho	IL1RN rho
Th1	0.296**	0.379**	0.43**	-0.106	0.12	0.003
Th2	0.144	0.045	0.149	0.266**	0.376**	0.056
Th17	-0.166*	0.012	-0.176*	-0.068	-0.232**	-0.048
Memory B cells	0.01	-0.182*	0.364**	0.006	-0.189*	0.015
Naïve B cells	-0.034	0.091	0.338**	-0.045	-0.06	-0.196*
Macrophages	0.204*	-0.071	-0.085	0.056	0.193*	0.23
M0	0.231**	-0.146	0.264**	-0.005	0.113	0.144
M1	0.074	-0.015	-0.053	-0.03	0.027	0.071**
M2	0.081	-0.064	0.06	0.087	0.137	0.274*
Plasma B cells	-0.146	-0.166*	-0.193*	-0.077	-0.192*	-0.189
Activated CD4 T cells	0.072	0.06	0.189*	-0.029	0.101	-0.05
Resting CD4 T cells	-0.09	0.186*	0.211**	0.014	-0.008	0.017
Naïve CD4 T cells	0.059	-0.042	-0.077	0	-0.025	-0.083*
CD8 T cells	-0.153	0.008	0.214**	-0.107	-0.159	-0.187
Follicular T cells	0.003	-0.104	-0.157	-0.129	-0.095	-0.11
Gamma T cells	0.032	0.134	-0.038	-0.04	-0.173*	-0.156
T regulatory cells	0.045	0.162*	-0.161*	-0.024	-0.176*	0.006**
Lymphocytes	-0.157	0.02	-0.028	-0.113	-0.264**	-0.234
Neutrophils	0.206*	0.279**	0.156	0.111	0.209**	0.049*
Eosinophils	0.234**	0.029	0.181*	0.165*	0.26**	0.176
Mast cells	-0.198*	-0.012	0.196*	0.104	0.012	0.026
Dendritic cells	-0.042	0.142	0.211**	0.123	0.222	0.039**

within the peripheral blood. No significant associations were found between local IL-1 α and IL-1Ra protein levels and the circulating immunophenotype (Table 3).

Table 3

Correlations between the tumor immune microenvironment and peripheral immunophenotype. Green coloring emphasizes increase, red emphasizes decrease, * signifies $p < 0.05$ and ** signifies $p < 0.01$.

	IL1A rho	IL1B rho	IL1RN rho
IL1A	1	0.830**	0.809**
IL1B	0.830**	1	0.533
IL1RN	0.809**	0.533	1
MDSC	0.097	0.157	-0.085
PDL1 gMFI	0.015	0.448	0.021
CD80 gMFI	-0.018	0.147	0.029
DC	-0.039	0.27	-0.082
CD4	0.171	0.168	0.188
CD8	-0.179	-0.196	-0.179
CD4 CM	0.184	0.626*	0.074
CD4 Eff	-0.377	-0.536	-0.074
CD4 EM	-0.107	-0.173	-0.161
CD4 Naïve	0.066	-0.297	0.189
Th1	0.132	-0.147	0.004
Th1.17	0.062	0.28	-0.197
Th17	-0.212	0.203	-0.244
Th0	-0.153	-0.231	0.068
Th2	-0.2	-0.65*	-0.044
CD8 CM	0.093	0.566*	0.031
CD8 Eff	-0.015	-0.132	-0.039
CD8 EM	0.308	0.305	0.335
CD8 Naïve	-0.027	0.264	-0.088

Immune checkpoint proteins

To assess the relationship between the IL-1 axis and potentially targetable immune checkpoint proteins, gene expression of the IL-1 axis was compared to the gene expression of PVR (CD155 protein), CD274 (Programmed death-ligand 1 protein), PDCD1 (program cell death 1 protein), CD47 (CD47 protein), CD80 (CD80 protein), CD86 (CD86 protein), HLA A/B/C (MHC class 1 molecules), CTLA4 (CTLA-4 protein), and IDO1 (Indoleamine 2,3-dioxygenase 1 protein) (Fig. 3). Increased gene expression of all of the aforementioned immune checkpoint inhibitors ($p \leq 0.002$). Additionally, IL1A, IL1RN and IL1RAP expression, those increased in

PDAC samples, corresponded to an increased expression of PVR, CD47, CD80, HLAA, HLAB, and HLAC ($p < 0.05$). Moreover, IL1A ($p = 0.002$) and IL1RAP ($p = 0.001$) were associated with increased expression of CD274. IL1RAP was also found to be associated with increased expression of IDO1 ($p = 0.001$). Alternatively, the gene expression of IL1R2 was only correlated with increased expression of PVR ($p = 0.001$) and HLA A ($p = 0.016$).

Patient survival

To delineate how the gene expression of the IL-1 axis impacts patient survival in PDAC, high and low expression groups were compared (Fig. 4). Patients with low tumor expression of IL1B experienced decreased overall survival when compared to those with high expression ($p = 0.031$, 17.7 vs. 30.4 months). Decreased overall survival was also found in patients with high tumor expression of the antagonists IL1R2 ($p = 0.015$, 9.2 vs. 20.2 months) and IL1RN ($p = 0.02$, 18.2 vs. 44.4 months). Furthermore, high expression of IL1RAP was associated with decreased overall survival ($p = 0.003$, 16.6 vs. 23.4 months). No statistically significant differences in patient survival were found between high and low expression of IL1A ($p = 0.084$, 18.9 vs. 22.0 months) and IL1R1 ($p = 0.139$, 20.2 vs. 16.6 months).

Discussion

The findings of this study indicate that the IL-1 axis is implicated in PDAC biology, including the host tumor immune microenvironment, and in patient overall survival. Patients with PDAC have increased IL1A (encoding the protein IL-1 α), IL-1RN (encoding for IL-1Ra), IL1R2 (encoding for the decoy receptor IL-1R₂) and IL1RAP (encoding for the accessory protein IL-1R₃) when compared to benign tissue. Further supporting these findings, DNA methylation of IL1A, IL1RN, IL1R2, IL1RAP as well as IL1B (encoding for IL-1 β) was decreased in PDAC samples. Given that DNA methylation often leads to gene repression through transcription inhibition, these findings indicate that this mechanism may contribute to PDAC tumorigenesis.

Furthermore, the IL-1 axis in PDAC is correlated with significant changes in the tumor immune landscape as well as the expression of tumor immune checkpoint proteins. This study is the first of its kind to assess how tumor immune checkpoint expression in human PDAC patient samples are correlated with expression of the IL-1 family members. Moreover, it assesses the correlation between IL-1 soluble proteins in the tumor microenvironment and the peripheral immune response. Though a limited number of patient samples were available for analysis, the peripheral immunophenotype does not appear to be representative of the local tumor immune response. The peripheral immunophenotype shows evidence of IL-1 β correlation with increased central memory CD4⁺ and CD8⁺ T-cells and decreased Th2 cells, though this is not recapitulated in the tumor immune microenvironment expression data. Interestingly, patients with low tumor expression of IL1B and high expression of IL1RN and IL1R2 experienced decreased overall survival in PDAC. These findings are particularly important to consider when manipulating the IL-1 axis for potential cancer therapeutics.

There are currently several early phase clinical trials targeting the IL-1 axis specifically in PDAC. Anakinra, the recombinant IL-1Ra protein, in combination with pre-operative and post-operative chemotherapy is in phase 2 clinical trial for PDAC (NCT 04926467) [22]. In preclinical models, Zuang et al. found that the use of anakinra abrogated tumor growth through a decrease in NF- κ B activation. They further utilized genetically-engineered IL-1 α ^{-/-} mice to show that without IL-1 α , tumors exhibited decreased growth and decreased phosphorylated EGFR, phosphorylated ERK, cyclin D1, and Ki67 [13].

Additionally, Xilonix (XBiotech), an anti-IL-1 α monoclonal antibody, in combination with nanoliposomal irinotecan and 5-fluorouracil, folinic

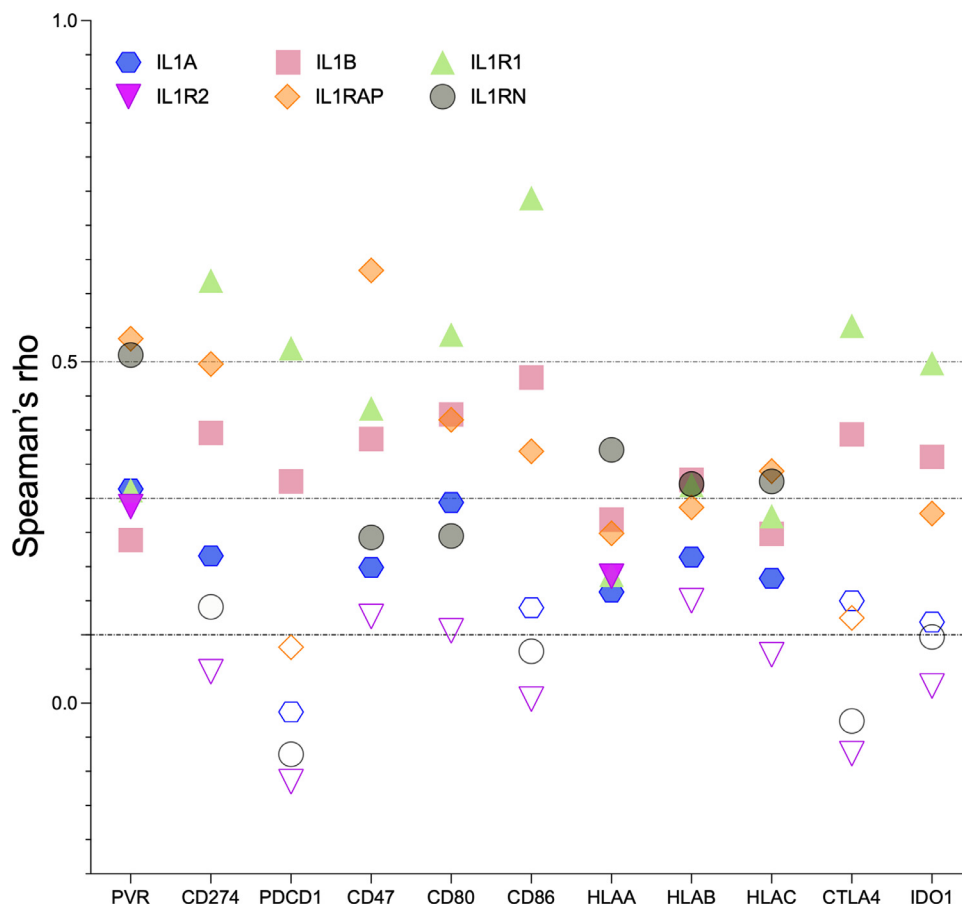


Fig. 3. Spearman two-tailed correlations of the IL-1 family (IL1A, IL1B, IL1R1, IL1R2, IL1RAP, IL1RN) and immune checkpoint proteins in 169 TCGA-PAAD samples. Solid shapes signify p -value < 0.05 .

acid has completed phase 1 clinical trial in PDAC, though results are not currently publicly available (NCT03207724) [23]. In preclinical *in vitro* models, Tjomsland et al. found that IL-1 α initiates the production of inflammatory factors, including COX-2, IL-6, and CXCL8, through its binding to IL-1R $_1$ found primarily on cancer-associated fibroblasts (CAFs) [24]. Furthermore, Biffi et al. utilized both organoid and murine models to explore how tumor-secreted IL-1 α generates inflammatory CAFs through the induction of leukemia inhibitory factor (LIF) expression and downstream JAK/STAT activation [25]. Despite these interesting findings, the impact of IL-1 inhibition on the tumor immune landscape and immune checkpoint proteins in PDAC patients remains largely unknown.

A phase 1B clinical trial studying the use of canakinumab, a high-affinity human anti-IL-1 β monoclonal antibody and spartalizumab, an anti PD-1 monoclonal antibody, in combination with chemotherapy is currently active for PDAC patients (NCT04581343) [26]. In preclinical models, Das et al. found that tumor cell-derived IL-1 β led to the establishment of an immunosuppressive tumor microenvironment mediated by M2 macrophages, myeloid-derived suppressor cells, CD1d(hi)CD5+ regulatory B cells, and Th17 cells [27]. Further, they found that antibody-mediated neutralization of IL-1 β led to improved utility of anti-PD-1 antibodies in promoting increased infiltration of CD8+ T-cells. The results of our study further support these findings showing significant positive correlation between IL1B and PDCDI, which encodes the protein PD-1, as well as CD274, which encodes for its ligand PD-L1 [27]. However, contrary to their findings, IL1B was not found to be significantly correlated with

M2 macrophages or Th17 cells in our study, though this difference may be attributable to a static vs. dynamic assessment of the PDAC tumor microenvironment.

The results of this study provide a more comprehensive understanding of the impact of the IL-1 axis on the tumor immune microenvironment, immune checkpoint proteins and overall survival in human PDAC patients. This is particularly important as this axis is manipulated in targeted cancer therapeutics that are aimed at decreasing the impact of IL-1 α and IL-1 β through monoclonal antibodies or recombinant IL-1Ra. However, our data alternatively show that high IL1B and low IL1RN expression is correlated with improved survival. This may be a result of the downstream impact on the tumor immune landscape as well as immune checkpoint proteins. Furthermore, as the IL-1 axis is evaluated as a therapeutic target, additional consideration should be given to its influence on the tumor immune landscape and immune checkpoint proteins for potential combination therapies.

This study has several limitations. It is a retrospective database analysis and as such is limited to the data provided through TCGA and GEO. Further, it utilizes a bioinformatics approach to assess gene expression and methylation data, which presents a static picture of gene expression instead of dynamic interactions seen in the complex tumor microenvironment. An additional limitation of the analysis is the lack of metastatic tumors, where therapies targeting IL-1 are likely to be employed. Furthermore, though CIBERSORTx is a well-established tool, the immune cell compositions are only estimations based on gene expression.

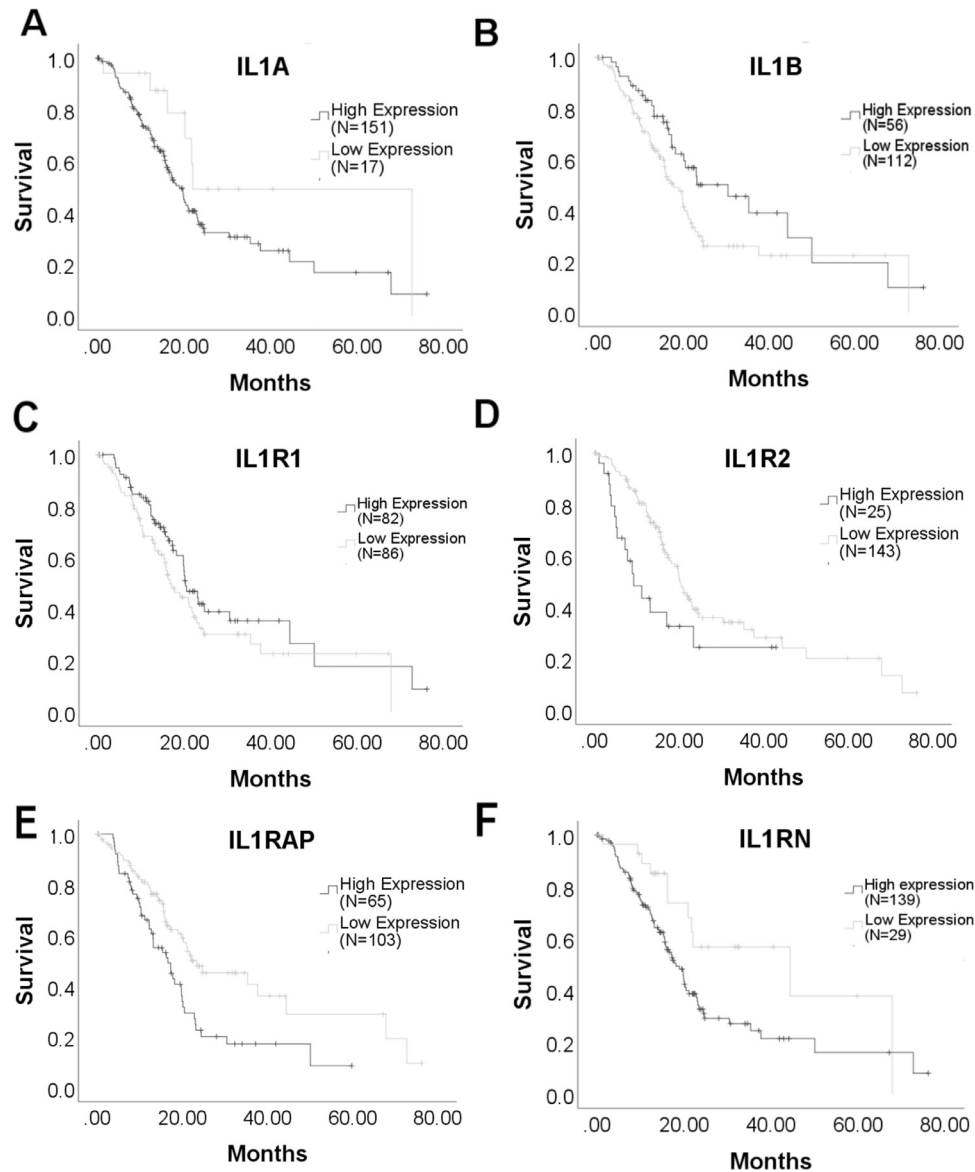


Fig. 4. Kaplan Meier analysis of high vs. low expression of IL1A, IL1B, IL1RN, IL1R1, IL1R2, IL1RAP, using Cutoff Finder. * denotes significance of p -value <0.05 and ** denotes significance of p -value <0.01 .

Conclusions

This study is the first of its kind to evaluate the impact of the totality of the IL-1 axis on the tumor immune microenvironment in patients with PDAC. It highlights the changes in IL1A, IL1B, IL1RN, IL1R1, IL1R2 and IL1RAP expression in PDAC and further explores the impact on the immune landscape and immune checkpoint proteins. These findings provide value to the design and interpretation of ongoing exploration of the IL-1 axis as a therapy for patients with PDAC. Further, these findings suggest that manipulation of the IL-1 axis in combination with immune checkpoint proteins may be warranted.

Funding

This work is supported by the National Human Genome Research Institute (T32 HG0008958 to KMH and ANR) and National Cancer

Institute and National Institute of Diabetes and Digestive and Kidney Diseases of the National Institutes of Health under award number 1U01DK108320 (SJH). The content is solely the responsibility of the authors and does not necessarily represent the official views of the National Institutes of Health.

Declaration of Competing Interest

The authors declare that they have no known competing financial interests or personal relationships that could have appeared to influence the work reported in this paper.

CRedit authorship contribution statement

Kelly M. Herremans: Conceptualization, Methodology, Formal analysis, Writing – original draft. **Dominique D. Szymkiewicz:** Conceptualization,

Methodology, Software, Writing – original draft. **Andrea N. Riner:** Conceptualization, Writing – review & editing. **Riley P. Bohan:** Conceptualization, Writing – review & editing. **Gerik W. Tushoski:** Visualization, Writing – review & editing. **Aaron M. Davidson:** Conceptualization, Writing – review & editing. **XiangYang Lou:** Software, Data curation, Writing – review & editing. **Man Chong Leong:** Software, Data curation, Writing – review & editing. **Song Han:** Methodology, Formal analysis, Visualization, Writing – review & editing. **Steven J. Hughes:** Conceptualization, Methodology, Resources, Visualization, Writing – review & editing, Supervision.

Acknowledgments

The results published here are in whole or part based upon data generated by the TCGA Research Network: <https://www.cancer.gov/tcga>.

Supplementary materials

Supplementary material associated with this article can be found, in the online version, at doi:10.1016/j.neo.2022.100789.

References

- [1] Singh RR, O'Reilly EM. New treatment strategies for metastatic pancreatic ductal adenocarcinoma. *Drugs* 2020;**80**(7):647–69. doi:10.1007/s40265-020-01304-0.
- [2] Survival Rates for Pancreatic Cancer. American Cancer Society. <https://www.cancer.org/cancer/pancreatic-cancer/detection-diagnosis-staging/survival-rates.html>. (Accessed Oct. 17, 2021)
- [3] Bergholz JS, Wang Q, Kabraji S, et al. Integrating immunotherapy and targeted therapy in cancer treatment: mechanistic insights and clinical implications. *Clin Cancer Res.* 2020;**26**(21):5557–66 Nov 1Epub 2020 Jun 23. doi:10.1158/1078-0432.CCR-19-2300.
- [4] Ralli M, Borticelli A, Visconti IC, et al. Immunotherapy in the treatment of metastatic melanoma: current knowledge and future directions. *J Immunol Res* 2020;**2020**:9235638. doi:10.1155/2020/9235638.
- [5] Delitto D, Waller SM, Hughes SJ. Targeting tumor tolerance: a new hope for pancreatic cancer therapy? *Pharmacol Ther* 2016;**166**:9–29 Oct. doi:10.1016/j.pharmthera.2016.06.008.
- [6] Mace TA, Ameen Z, Collins A, et al. Pancreatic cancer-associated stellate cells promote differentiation of myeloid-derived suppressor cells in a STAT3-dependent manner. *Cancer Res.* 2013;**73**(10):3007–18 May 15Epub 2013 Mar 20. doi:10.1158/0008-5472.CAN-12-4601.
- [7] Sanford DE, Belt BA, Panni RZ, et al. Inflammatory monocyte mobilization decreases patient survival in pancreatic cancer: a role for targeting the CCL2/CCR2 axis. *Clin Cancer Res* 2013;**19**(13):3404–15 Jul 1Epub 2013 May 7. doi:10.1158/1078-0432.CCR-13-0525.
- [8] Mantovani A, Dinarello CA, Molgora M, et al. Interleukin-1 and related cytokines in the regulation of inflammation and immunity. *Immunity* 2019;**50**(4):778–95. doi:10.1016/j.immuni.2019.03.012.
- [9] Litmanovich A, Khazim K, Cohen I. The role of interleukin-1 in the pathogenesis of cancer and its potential as a therapeutic target in clinical practice. *Oncol Ther* 2018;**6**:109–27. doi:10.1007/s40487-018-0089-z.
- [10] Baker KJ, Houston A, Brint E. IL-1 family members in cancer; two sides to every story. *Front Immunol.* 2019;**10**:1197 Jun 7. doi:10.3389/fimmu.2019.01197.
- [11] Underwood PW, Gerber MH, Nguyen K, et al. Protein signatures and tissue diagnosis of pancreatic cancer. *J Am Coll Surg* 2020;**230**(1):26–36 Jan.e1. doi:10.1016/j.jamcollsurg.2019.10.002.
- [12] Delitto D, Black BS, Sorenson HL, et al. The inflammatory milieu within the pancreatic cancer microenvironment correlates with clinicopathologic parameters, chemoresistance and survival. *BMC Cancer* 2015;**15**(2015):783. doi:10.1186/s12885-015-1820-x.
- [13] Zhuang Z, Ju HQ, Aguilar M, et al. IL1 receptor antagonist inhibits pancreatic cancer growth by abrogating NF- κ B activation. [published correction appears in *Clin Cancer Res.* 2017 Feb 1;**23**(3):868]. *Clin Cancer Res.* 2016;**22**(6):1432–44. doi:10.1158/1078-0432.CCR-14-3382.
- [14] Whiteley A, Becerra C, McCollum D, et al. MA pilot, non-randomized evaluation of the safety of anakinra plus FOLFIRINOX in metastatic pancreatic ductal adenocarcinoma patients. *J Clin Oncol* 2016;**34**(15_suppl):e15750 -e15750.
- [15] Edgar R, Domrachev M, Lash AE. Gene expression omnibus: NCBI gene expression and hybridization array data repository. *Nucleic Acids Res* 2002;**30**(1):207–10 Jan 1.
- [16] Pei H, Li L, Fridley BL, Jenkins GD, et al. FKBP51 affects cancer cell response to chemotherapy by negatively regulating Akt. *Cancer Cell* 2009;**16**(3):259–66 Sep 8.
- [17] Zhang G, Schetter A, He P, et al. DPEP1 inhibits tumor cell invasiveness, enhances chemosensitivity and predicts clinical outcome in pancreatic ductal adenocarcinoma. *PLoS One* 2012;**7**(2):e31507.
- [18] Thorsson V, Gibbs DL, Brown SD, et al. The immune landscape of cancer. [published correction appears in *Immunity.* 2019 Aug 20;**51**(2):411–412]. *Immunity* 2018;**48**(4):812–30 .e14. doi:10.1016/j.immuni.2018.03.023.
- [19] Newman AM, Liu CL, Green MR, et al. Robust enumeration of cell subsets from tissue expression profiles. *Nat Methods* 2015;**12**(5):453–7. doi:10.1038/nmeth.3337.
- [20] Finak G, Langweiler M, Jaimes M, et al. Standardizing flow cytometry immunophenotyping analysis from the human immunophenotyping consortium. *Sci Rep* 2016;**6**:20686. doi:10.1038/srep20686.
- [21] Budczies J, Klauschen F, Sinn BV, et al. Cutoff Finder: a comprehensive and straightforward Web application enabling rapid biomarker cutoff optimization. *PLoS One* 2012;**7**(12):e51862. doi:10.1371/journal.pone.0051862.
- [22] Becerra C. (June 15, 2021-). Chemotherapy + anakinra in patients with pancreatic adenocarcinoma (PDAC). Identifier NCT04926467. <https://clinicaltrials.gov/ct2/show/NCT04926467> (Accessed Oct. 30, 2021).
- [23] Hendifar A. (July 5, 2017- December 30, 2020). Study of onivyde and 5-FU in combination with xilonix for pancreatic cancer with cachexia (OnFX). Identifier NCT03207724. <https://clinicaltrials.gov/ct2/show/NCT03207724> (Accessed Oct. 30, 2021).
- [24] Tjomsland V, Spångaus A, Väilä J, et al. Interleukin 1 α sustains the expression of inflammatory factors in human pancreatic cancer microenvironment by targeting cancer-associated fibroblasts. *Neoplasia* 2011;**13**(8):664–75 Aug. doi:10.1593/neo.11332.
- [25] Biffi G, Oni TE, Spielman B, et al. IL1-induced JAK/STAT signaling is antagonized by TGF β to shape CAF heterogeneity in pancreatic ductal adenocarcinoma. *Cancer Discov* 2019;**9**(2):282–301. doi:10.1158/2159-8290.CD-18-0710.
- [26] Deck R. (October 9, 2020 -) A phase 1B study of canakinumab, spartalizumab, nab-paclitaxel, and gemcitabine in metastatic PC patients (PanCAN-SR1). Identifier NCT04581343. <https://clinicaltrials.gov/ct2/show/NCT04581343> (Accessed Oct. 30, 2021).
- [27] Das S, Shapiro B, Vucic EA, et al. Tumor cell-derived IL1 β promotes desmoplasia and immune suppression in pancreatic cancer. *Cancer Res* 2020;**80**(5):1088–101 Mar 1. doi:10.1158/0008-5472.CAN-19-2080.